

Study of electrical and optical properties of $\text{Cd}_{1-x}\text{Zn}_x\text{S}$ thin films

M. A. REDWAN

University College for Art, Science and Education, Ain Shams University, Cairo, Egypt
E-mail: sdeeb@main-scc.cairo.eun.eg

L. I. SOLIMAN

National Research Center, Cairo, Egypt

E. H. ALY, A. A. EL-SHAZELY, H. A. ZAYED

University College for Art, Science and Education, Ain Shams University, Cairo, Egypt

Thin films of $\text{Cd}_{0.9}\text{Zn}_{0.1}\text{S}$ and CdS were prepared by thermal evaporation under vacuum of 10^{-6} Torr and with deposition rate of 60 nm/min. X ray diffraction studies confirm the hexagonal structure of both CdS and $\text{Cd}_{0.9}\text{Zn}_{0.1}\text{S}$ films. The effect of heat treatments with or without CdCl_2 enhances the grain size growth and improves the crystalline of the films. Moreover, the activation energy is decreased by heat treatment with or without CdCl_2 for all thin films. The optical absorption coefficient of $\text{Cd}_{0.9}\text{Zn}_{0.1}\text{S}$ thin films were determined from measured transmittance and reflectance in the wavelength range of 300 to 2500 nm. The optical absorption spectra reveal the existence of direct energy gap for these films. It was found that the optical energy gap decreases upon annealing or CdCl_2 treatments. © 2003 Kluwer Academic Publishers

1. Introduction

The growth and characterization of CdS , ZnS and $\text{Cd}_{1-x}\text{Zn}_x\text{S}$ thin films have received great attention due to their photovoltaic potential [1–3]. Most of the electrical and optical properties of these films can be controlled by proper choice of the growth parameters, growth method, and the post deposition treatment. Generally, CdS and ZnS from solid solutions over the entire composition range from $x = 0$ to $x = 1$ [4, 5]. The alloy films exist in a single-phase wurtzite structure. Alloy $\text{Cd}_{1-x}\text{Zn}_x\text{S}$ films with $x = 0.1$ [i.e., $\text{Cd}_{0.9}\text{Zn}_{0.1}\text{S}$] have been prepared from a mixture of the compounds, CdS and ZnS by different preparation techniques [5–8]. The value of x for $\text{Cd}_{1-x}\text{Zn}_x\text{S}$ films plays an important role in determining their structural, electrical, and optical properties. Due to the rapid increase in the resistivity of $\text{Cd}_{1-x}\text{Zn}_x\text{S}$ with increasing x value, the range of useable composition for solar cell applications is limited to values of $x < 0.2$ [9]. Fractional content of Zn with $x = 0.1$ ($\text{Cd}_{0.9}\text{Zn}_{0.1}\text{S}$) in the $\text{Cd}_{1-x}\text{Zn}_x\text{S}$ films is maintained in the present study.

The present work deals with the determination of lattice parameters; conductivity and the optical constants of $\text{Cd}_{0.9}\text{Zn}_{0.1}\text{S}$ thin films, as well as the investigation of the crystallization of $\text{Cd}_{0.9}\text{Zn}_{0.1}\text{S}$ with annealing at about 673 K with or without CdCl_2 treatment.

2. Experimental

2.1. Preparation of the thin films

Thin films of $\text{Cd}_{0.9}\text{Zn}_{0.1}\text{S}$ and CdS were prepared by the conventional thermal evaporation technique using

a Leybal-Heraeus high vacuum coating unit of type Univex-300 provided with INFICON XTC, thin film thickness and rate controller. CdS and $\text{Cd}_{0.9}\text{Zn}_{0.1}\text{S}$ films with a thickness of 200 nm were deposited with a deposition rate of 60 nm/min. and at substrate temperature $T_s = 423$ K. To examine the effect of post deposition treatments, some films were heat treated with CdCl_2 vapor. The treatments were performed by exposing the $\text{Cd}_{0.9}\text{Zn}_{0.1}\text{S}$ films to a vapor generated from a powder CdCl_2 source in two-zone tube furnace. To prevent CdCl_2 condensation on the samples, the films were heated prior to and cool after the exposure to the CdCl_2 treatment. The treatments were conducted under flowing gas (N_2) at total pressure of one atmosphere and the system was roughly pumped prior to the back filling. During the heat-treatments, the samples were held at 673 K and the CdCl_2 source was held at 573 K for 20 min. The heat-treatment step was followed by rinse in distilled deionized water to remove any traces of residual CdCl_2 coating.

2.2. X-ray diffraction (XRD)

The XRD patterns of $\text{Cd}_{0.9}\text{Zn}_{0.1}\text{S}$ and CdS samples for both the powder and the thin films deposited on glass substrates were recorded using Philips PW 1373 X-ray diffractometer, with nickel filtered Cu K_α radiation of wavelength $\lambda = 1.5418$ Å. The diffraction patterns were recorded automatically with scanning speed of 2 degrees per minute. The XRD investigations included the effect of heat and CdCl_2 treatments on the structure of the examined films.

2.3. Optical measurements

The transmittance $T(\lambda)$ and reflectance $R(\lambda)$ of the as-deposited and post-treated films were measured by using JASCO model V-570 UV-VIS-NIR double beam spectrophotometer with a wavelength range from 300 to 2500 nm.

2.4. Electrical measurements

Electrical resistivity measurements of the prepared thin films were performed by the coplanar two-probe technique in the temperature range from 300 K to 500 K, using Keithley 616 digital electrometer. Hall effect measurements were carried out by the traditional DC method for the Hall voltage, using a uniform magnetic field of about 9 K Orested. The experimental errors were estimated to be in the order of 3%.

3. Results and discussion

3.1. Structural properties

XRD patterns of thermally evaporated $\text{Cd}_{0.9}\text{Zn}_{0.1}\text{S}$ films on glass substrate with different treatments: (A) as-deposited, (B) annealed in nitrogen (N_2) atmosphere at 673 K for 20 min. and (C) treated with CdCl_2 vapor at 673 K for 20 min are shown in Fig. 1. The pattern shown that all films have hexagonal structure with strong (002) peak, indicating that the crystallites are preferentially oriented with their c-axis perpendicular to the surface. The calculated lattice parameters a and c were $4.105 \pm 0.008 \text{ \AA}$ and $6.673 \pm 0.008 \text{ \AA}$ respectively. The obtained results compare well with the reported one [1, 10, 11]. The composition parameter x of the $\text{Cd}_{0.9}\text{Zn}_{0.1}\text{S}$ films was determined by assuming a linear variation of the lattice constants, which is a convenient method to obtain the value of x easily from XRD measurements [1, 12]. The x value can be obtained by substituting the calculated values for the lattice parameters a and c in

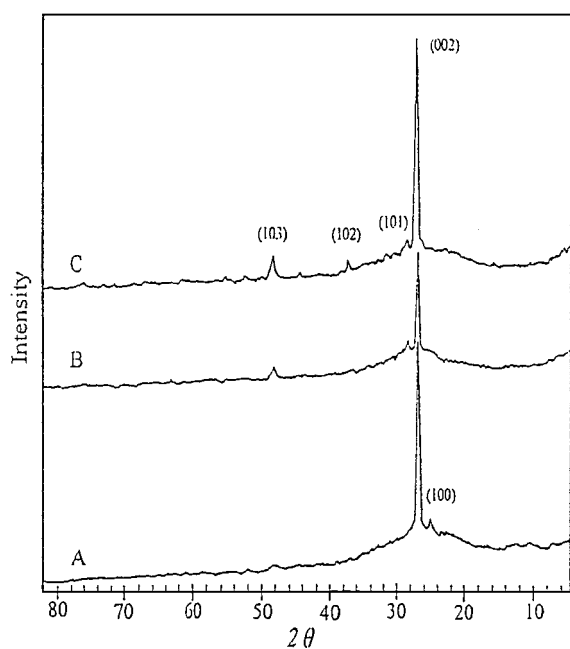


Figure 1 XRD patterns for $\text{Cd}_{0.9}\text{Zn}_{0.1}\text{S}$ films, as deposited (A), annealed for 20 min at 673 K (B) and CdCl_2 treated at 673 K for 20 min (C).

the following equations [13]

$$a = 4.1370 - 0.3165x \quad (1)$$

$$c = 6.7168 - 0.4597x \quad (2)$$

The value of x is found to be 0.1, which is identical with the intended composition of prepared $\text{Cd}_{0.9}\text{Zn}_{0.1}\text{S}$ films and agrees with the results obtained by energy—dispersive X-ray analysis (EDX). For all films, as seen in Fig. 1, the (002) plane gives the strongest reflection. The as-deposited film pattern also shows a small reflection from the (100) plane. After film annealing at 673 K two subsidiary peaks of relatively low intensity corresponding to the (101) and (103) planes are also observed while the peak corresponds to (100) plane disappeared. For the films treated with CdCl_2 vapor an extra peak of the (102) plane appeared and all the observed peaks become sharper, relative to the annealed ones see Fig. 1c.

The grain size L was estimated from the (002) peak using the Scherrer formula [14]

$$L = K\lambda/\beta \cos \theta \quad (3)$$

where β is the full width at half maximum of the diffraction peak located at angle 2θ and K is Scherrer's constant which approximately equal unity. The calculated values of the lattice parameters as well as the values of L are presented in Table I. The slow rate deposition of $\text{Cd}_{0.9}\text{Zn}_{0.1}\text{S}$ films yields as-deposited films with a large grain size. $\text{Cd}_{0.9}\text{Zn}_{0.1}\text{S}$ films annealed at 673 K without CdCl_2 show the corresponding smaller grain size. These effects can be attributed to the sulfur loss from the film surface, which in turn leads to increase the density of structural defects. The presence of CdCl_2 during heat treatment at 673 K prevents sulfur loss from the surface, hence, the structural defect density is lowered the grain growth is enhanced, and the film crystallinity is improved as seen in Fig. 1 and Table I. It worth mentioning that the X-ray photoelectron spectroscopy (XPS) examination of CdS films [15] showed that films treated at 823 K without CdCl_2 exhibited sever sulfur loss from the surface region while no such loss was detected upon using CdCl_2 .

For the comparison purpose, CdS films were prepared at the same conditions and subjected to similar treatments as $\text{Cd}_{0.9}\text{Zn}_{0.1}\text{S}$ films. The obtained XRD

TABLE I Calculated lattice parameters and average grain size of $\text{Cd}_{0.9}\text{Zn}_{0.1}\text{S}$ and CdS films with different treatments

Sample	Lattice parameters		Average grain size L (Å)
	a (Å)	c (Å)	
$\text{Cd}_{0.9}\text{Zn}_{0.1}\text{S}$ films			
As deposited	4.097 ± 0.005	6.677 ± 0.005	290
Annealed	4.114 ± 0.005	6.674 ± 0.005	270
CdCl_2 treated	4.112 ± 0.005	6.678 ± 0.005	340
CdS films			
As deposited	4.134 ± 0.005	6.731 ± 0.005	390
Annealed	4.153 ± 0.005	6.725 ± 0.005	344
CdCl_2 treated	4.153 ± 0.005	6.731 ± 0.005	430

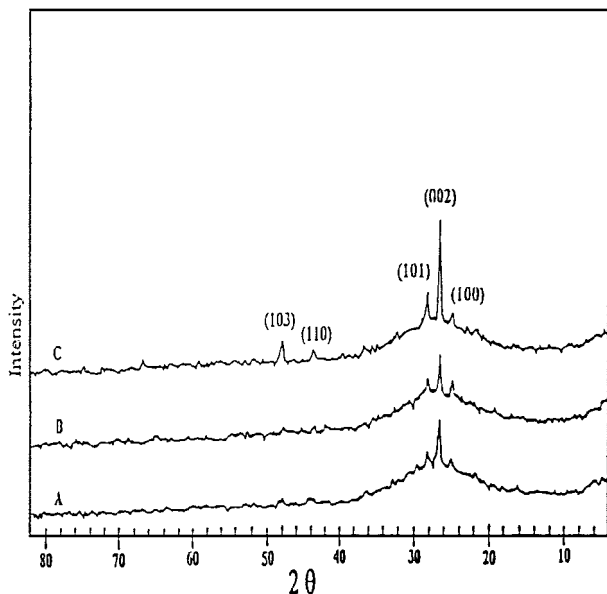


Figure 2

patterns for CdS films shown in Fig. 2 agree well with the data of the standard JCPDS card. The calculated lattice parameters and the average grain size of CdS films are summarized in Table I. By comparing the XRD patterns of $\text{Cd}_{0.9}\text{Zn}_{0.1}\text{S}$ films and CdS films, it is found that, they have the hexagonal structure and similar properties. The position of diffraction peaks of $\text{Cd}_{0.9}\text{Zn}_{0.1}\text{S}$ films is shifted toward higher 2θ compared with that of CdS films. A decrease in the lattice constants of $\text{Cd}_{0.9}\text{Zn}_{0.1}\text{S}$ films is expected due to the increase in the diffraction angle.

Finally, it can be concluded that $\text{Cd}_{0.9}\text{Zn}_{0.1}\text{S}$ films are hexagonal polycrystalline with large grain size when obtained by CdCl_2 treatment at 673 K for 20 min. Moreover, CdCl_2 treatment improves the $\text{Cd}_{0.9}\text{Zn}_{0.1}\text{S}$ films crystallinity. Hence, it minimizes junction defects when the film is used as a window layer in $\text{Cd}_{0.9}\text{Zn}_{0.1}\text{S}/\text{CdTe}$ heterojunctions.

3.1.1. Electrical properties

The temperature dependence of the dark electrical conductivity σ is given by

$$\sigma = \sigma_0 \exp(-\Delta E/KT) \quad (4)$$

where σ_0 is the pre-exponential factor, ΔE is the activation energy of the electrical conduction, K is the Boltzmann's constant and T is the absolute temperature. The free carrier concentration (n) can be determined from Hall effect measurements ($n = 1/eR_H$) where e is the electronic charge and R_H is the Hall coefficient.

The Hall effect measurements and the thermoelectric power test for $\text{Cd}_{0.9}\text{Zn}_{0.1}\text{S}$ films in the temperature range from 300 K to 400 K indicate an n -type conduction. The temperature dependence of the dark electrical conductivity for the as deposited and as annealed $\text{Cd}_{0.9}\text{Zn}_{0.1}\text{S}$ and CdS films at 673 K for 20 min with and without CdCl_2 are shown in Figs 3 and 4. From these figures the following features can be noticed:

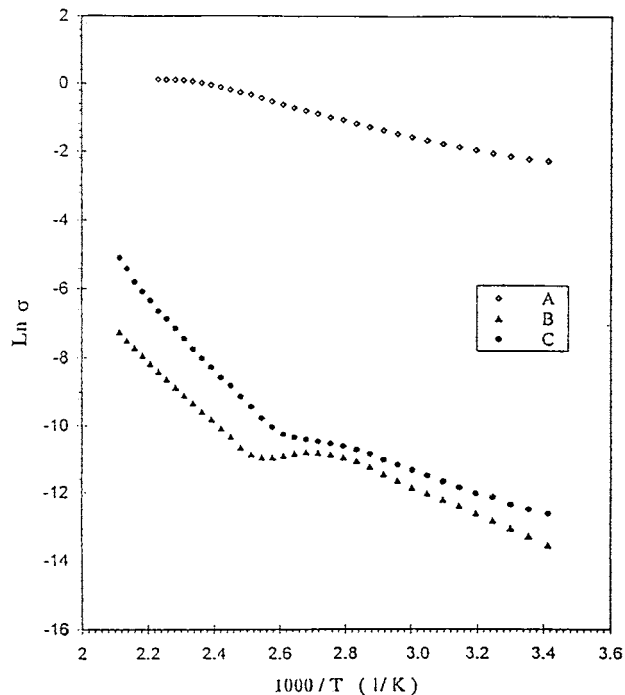


Figure 3 Temperature dependence of d.c. conductivity σ for $\text{Cd}_{0.9}\text{Zn}_{0.1}\text{S}$ films, as deposited (A), annealed for 20 min at 673 K (B) and CdCl_2 treated at 673 K for 20 min (C).

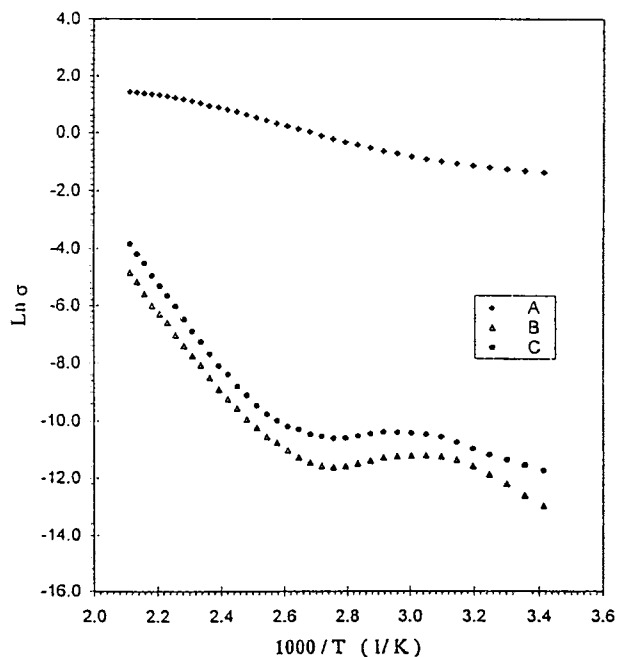


Figure 4

- The as-deposited and treated $\text{Cd}_{0.9}\text{Zn}_{0.1}\text{S}$ and CdS thin films have the same behavior of conductivity that increases with temperature, but the conductivity of the as-deposited and treated $\text{Cd}_{0.9}\text{Zn}_{0.1}\text{S}$ films is smaller than that of CdS films.

- Slow deposition rate of $\text{Cd}_{0.9}\text{Zn}_{0.1}\text{S}$ and CdS films yields films with high conductivity relative to the treated ones. The conductivity of the films decreased by 5 orders of magnitude after annealing at 673 K for 20 min.

- As seen in Figs 3 and 4, plots of $\text{Ln } \sigma$ vs. $1000/T$ show two linear regions. Both obey Equation 4, and the

TABLE II Activation energies ΔE_1 , ΔE_2 and conductivity σ in dark and under light, for $\text{Cd}_{0.9}\text{Zn}_{0.1}\text{S}$ and CdS films with different treatments

Sample	Activation energy		Conductivity σ ($\Omega \cdot \text{cm}$) ⁻¹	
	ΔE eV		Dark	Light
	ΔE_1	ΔE_2		
$\text{Cd}_{0.9}\text{Zn}_{0.1}\text{S}$ films				
As-deposited	0.187	0.223	1.02×10^{-4}	4.27×10^{-1}
Annealed	0.361	0.810	1.30×10^{-6}	3.38×10^{-4}
CdCl_2 treated	0.285	0.902	3.33×10^{-6}	1.69×10^{-2}
CdS films				
As-deposited	0.131	0.255	2.56×10^{-1}	5.42×10^{-1}
Annealed	0.397	1.103	2.33×10^{-6}	4.20×10^{-4}
CdCl_2 treated	0.259	1.130	8.00×10^{-6}	6.33×10^{-3}

rate of increase in conductivity in the high temperature region (370–450 K) is greater than that in the low temperature region (300–350 K). The electrical conduction activation energies at low temperature ΔE_1 and at high temperatures ΔE_2 are determined from the corresponding slopes of $\text{Ln } \sigma$ vs. $1000/T$ plots. Their values are listed in Table II with the corresponding room temperature dark and light conductivities.

– Activation energy values of the as-deposited films are smaller than those of annealed and treated films. The high conductivity and small activation energies of the as-deposited $\text{Cd}_{0.9}\text{Zn}_{0.1}\text{S}$ and CdS films may be attributed to both preferential orientation of the crystallites and the large grain size, as a result an enhancement in the free carriers mobility occurs. Annealing the films at 673 K reduces the grain size and the ordering of crystallites, which in turn leads to a decrease in the mobility and the conductivity. While, the influence of preferred orientation along the (002) direction and the increase of the grain size for films treated with CdCl_2 vapor at 673 K becomes dominant in the electrical transport leads to increase the conductivity relative to the annealed films as seen in Figs 3 and 4.

The observed variation in mobility with annealing and heat treatment with CdCl_2 may be interpreted by considering the various scattering mechanisms that limit the mobility of current carriers in polycrystalline films.

Assuming that these mechanisms are non-interacting, the mobility can be expressed as [10]

$$\mu^{-1} = \mu_g^{-1} + \mu_s^{-1} + \mu_b^{-1} \quad (5)$$

where the subscripts g , s and b refer to grain boundary, surface, and bulk crystal mechanisms, respectively. May *et al.* [16] derived a theoretical expression for μ_s as follows

$$\mu_s = \mu_k [1 + 2L/t] \quad (6)$$

where $\mu_k^{-1} = \mu_s^{-1} + \mu_b^{-1}$, L is the surface scattering length and t is the film thickness. For polycrystalline CdS films the value of $L = 1230 \text{ \AA}$ was determined experimentally [17] which agrees fairly well with the theoretically predicted value (1100 \AA), therefore $2L/t$ can be estimated to be 1.23 \AA for our films ($t = 2000 \text{ \AA}$),

independent of annealing temperature. For such value of $2L/t$ the effect of surface scattering on mobility is negligible [17]. The crystal bulk mobility μ_b may be affected by the ionized impurity scattering following variations in the doping level. However, for the large free carrier concentrations, (10^{17} cm^{-3}) this mechanism is thought to have a little effect on the carrier mobility of II–VI compounds at room temperature [10]. Therefore, it can be concluded that the grain boundary scattering is the primary mechanism that is responsible for the observed variation of μ with heat treatments. Such conclusion is in harmony with the obtained data for $\text{Cd}_{0.95}\text{Zn}_{0.05}\text{S}$ films [10].

Assuming that the inter-grain boundary materials take the form of a depletion barrier, Petritz [18] showed that the carrier mobility is thermally activated and it has the form

$$\mu = \mu_o \exp(-e\phi/KT) \quad (7)$$

where ϕ is the effective barrier height within the grain and μ_o is a constant which depends on the nature of the barrier and the linear grain boundary density, The value of ϕ can be calculated according to the following equation [19]

$$\phi = e^2 a^2 N_t / 4\epsilon a (1 - (n/[N_t/a]) \times \text{Ln}\{1 + [(N_t/a)/n]\}) \quad (8)$$

where a is the grain radius ($a = L/2$ where L is the grain size), n is the electron density, and N_t is the trap density. The value of ϕ can be estimated by plotting $\text{Ln } \mu$ vs. $1000/T$ as shown in Fig. 5. Consequently, the trap density N_t can be calculated.

Fig. 5 shows the behavior of μ with temperature for $\text{Cd}_{0.9}\text{Zn}_{0.1}\text{S}$ films with the different treatments.

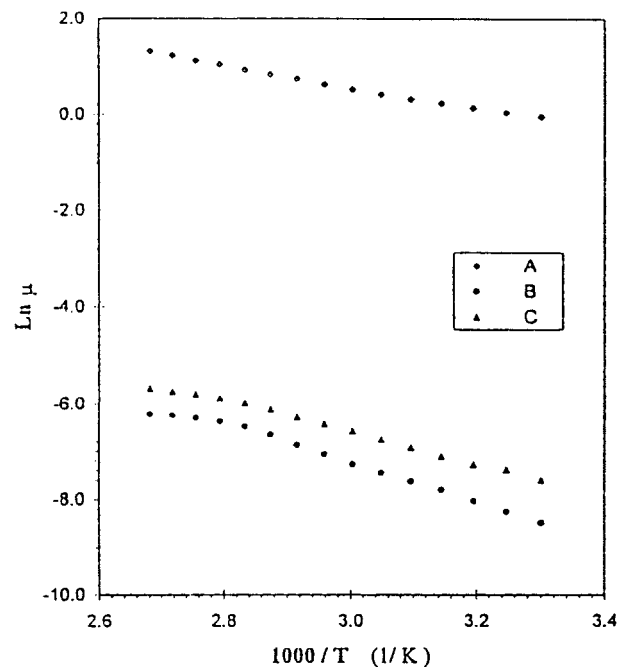


Figure 5 Temperature dependence of mobility μ for $\text{Cd}_{0.9}\text{Zn}_{0.1}\text{S}$ films, as deposited (A), annealed for 20 min 673 K (B) and CdCl_2 treated at 673 K for 20 min (C).

The values of ϕ and N_t as well as n for the as-deposited $\text{Cd}_{0.9}\text{Zn}_{0.1}\text{S}$ films ($T_s = 423$ K) compare fairly with the reported ones for the $\text{Cd}_{0.95}\text{Zn}_{0.05}\text{S}$ films deposited at $T_s = 623$ K [10]. Also, it is evident that both ϕ and N_t are increasing with increasing annealing temperature to 673 K, which leads to partial depletion of the grains. Consequently both μ and σ decrease significantly. For $\text{Cd}_{0.9}\text{Zn}_{0.1}\text{S}$ films treated with CdCl_2 (at 673 K for 20 min) $\phi = 0.267$ eV and $N_t = 9.8 \times 10^{11} \text{ cm}^{-3}$ are slightly decreasing leading to a little increase in the conductivity. This means that, the behavior of μ and n is related to the effect of partial depletion of the grains associated with the increase of inter-grain trap density.

It is noticed that $\text{Cd}_{0.9}\text{Zn}_{0.1}\text{S}$ films treated with CdCl_2 at 673 K for 20 min show high conductivity ($1.69 \times 10^{-2} \Omega^{-1} \text{ cm}^{-1}$) under illumination and the high light-to-dark conductivity ratio (5.08×10^3). The previous results suggest a long lifetime of the photo-generated majority carriers [20]. These results are in agreement with those obtained by Tang *et al.* [21] for CdS films.

Finally, it can be concluded that the electrical characteristics of the $\text{Cd}_{0.9}\text{Zn}_{0.1}\text{S}$ films make them appropriate as window layer for practical application in the photovoltaic field.

3.1.2. Optical properties

The study of the optical absorption in $\text{Cd}_{0.9}\text{Zn}_{0.1}\text{S}$ films, demonstrates the effect of different treatments on the optical properties and the density of defects in the films. The spectral distribution of both transmittance (T) and reflectance (R) in the wavelength range of 300–2500 nm for the as-deposited $\text{Cd}_{0.9}\text{Zn}_{0.1}\text{S}$ films, and for those annealed in nitrogen atmosphere at 673 K for 20 min with and without CdCl_2 are presented in Fig. 6. Transmission and reflection data of the all films show the same trend. The absorption coefficient $\alpha(h\nu)$ was calculated from $T(\lambda)$ and $R(\lambda)$ using the following relation [22]

$$T = [(1 - R^2 \exp(-\alpha t))/1 - R^2 \exp(-2\alpha t)] \quad (9)$$

where t is the film thickness.

The optical energy gap E_g is related to the absorption coefficient α for direct transition according to the equation [22]

$$\alpha h\nu = A(h\nu - E_g)^{1/2} \quad (10)$$

where A is a constant, h is the Plank's constant.

The optical band gap is obtained by plotting $(\alpha h\nu)^2$ as a function of photon energy ($h\nu$). Typical plots of $(\alpha h\nu)^2$ versus $(h\nu)$ for the as-deposited $\text{Cd}_{0.9}\text{Zn}_{0.1}\text{S}$ films as well for those heat treated for 20 minutes at 673 K with or without CdCl_2 are shown in Fig. 7. The values of the optical energy gap are estimated by extrapolating the linear portion of the curve to $(\alpha h\nu)^2 = 0$.

The calculated values of the optical energy gap for the as-deposited films are found to be equal to 2.48 eV, which agrees well with the calculated value for $\text{Cd}_{1-x}\text{Zn}_x\text{S}$ ($x = 0.1$) films grown by ion-beam de-

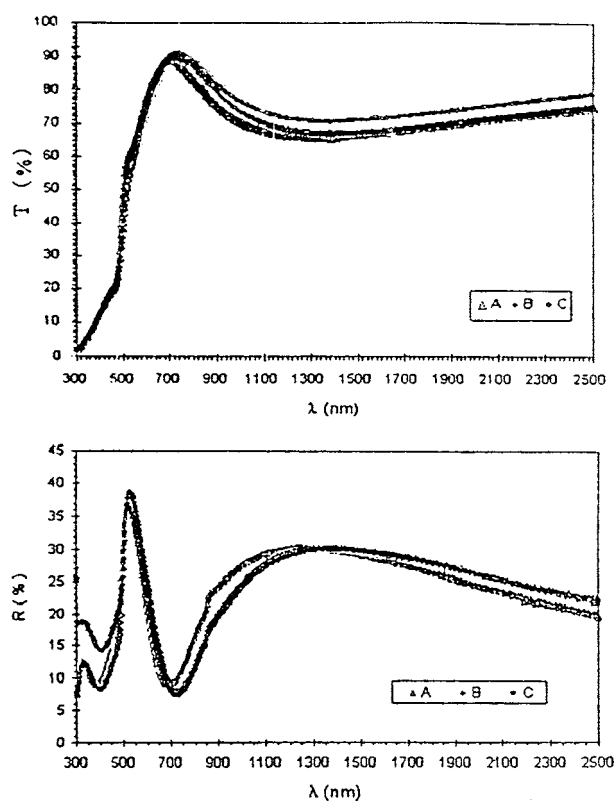


Figure 6 Spectral distribution of Transmittance (T) and Reflectance (R) for $\text{Cd}_{0.9}\text{Zn}_{0.1}\text{S}$ films, as deposited (A), annealed for 20 min at 673 K (B) and CdCl_2 treated at 673 K for 20 min (C).

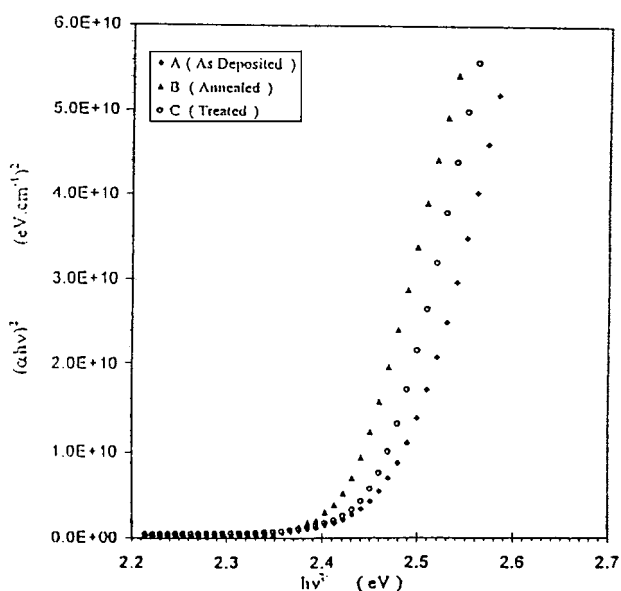


Figure 7 $(\alpha h\nu)^2$ vs. $h\nu$ for $\text{Cd}_{0.9}\text{Zn}_{0.1}\text{S}$ films, as deposited (A), annealed for 20 min at 673 K (B) and CdCl_2 treated at 673 K for 20 min (C).

position on glass substrates [1]. For films annealed at 673 K for 20 min the optical gap decreased to 2.43 eV. The decrease in the optical gap with annealing may be explained by the presence of high structure imperfection in the annealed films.

Upon the CdCl_2 treatment, the energy gap of the films was increased to 2.46 eV. This means that the defects responsible for the decrease in the optical gap are much less pronounced in films treated with CdCl_2 or as-deposited. Thus it can be concluded that CdCl_2

treatment is much more effective in improving the film properties than annealing. These results agree with the obtained measurements of the X-ray diffraction.

4. Conclusions

Thermally Cd_{0.9}Zn_{0.1}S films are polycrystalline with hexagonal structure. Heat treatment at 673 K for 20 min with or without CdCl₂ enhances the grain size growth and improves crystallinity of CdS and Cd_{0.9}Zn_{0.1}S thin films. Electrical conductivity σ of CdS and Cd_{0.9}Zn_{0.1}S films decreases by heat treatment with or without CdCl₂. Grain boundary scattering is the primary mechanism responsible for the observed behavior of electron mobility in Cd_{0.9}Zn_{0.1}S films.

Cd_{0.9}Zn_{0.1}S films are direct optical energy gap semiconductors. The variation of the optical gap with treatments can be explained by the presence of structure imperfections.

Generally it can be concluded that the electrical, the optical and the structural properties of Cd_{0.9}Zn_{0.1}S films make them good partner for CdTe to produce heterojunctions solar cells.

References

1. A. KUROYANAGI, *Thin Solid Films* **249** (1994) 91.
2. J. TORRES and G. GORDILLO, *ibid.* **207** (1992) 231.
3. K. SUBBARAMAIAH and V. SUNDRA RAJA, *Sol. Energy Mater. Sol. Cells* **32** (1994) 1.
4. J. A. RODRIGUEZ and G. GORDILLO, *Sol. Energy Mater.* **19** (1989) 421.
5. S. YAMAGA, A. YOSHIKAWA and H. KASSAI, *J. Crystal Growth* **99** (1990) 432.

6. M. P. SHOW, in "Handbook on Semiconductors" edited by T. S. Moss and C. Hilsum Vol. 4, Chap. 1 (Elsevier Science Publishers, North-Holland Amsterdam, 1993).
7. P. J. SEBSTIAN and M. OCAMPO, *Sol. Energy Mater. Sol. Cells* **44** (1996) 1.
8. T. EDAMURA and J. MUTO, *J. Mater. Sci. Lett.* **14** (1995) 889.
9. L. C. BURTON and T. L. HENCH, *Appl. Phys.* **29** (1976) 612.
10. F. EL AKKAD and M. ABDEL-NABY, *Sol. Energy Mater.* **17** (1988) 143.
11. G. C. MORRIS and R. VANDERVEN, *Sol. Energy Mater. Sol. Cells* **26** (1992) 217.
12. T. YOKOGAWA, T. ISHIKAWA and J. L. MERZ, *J. Appl. Phys.* **75** (1994) 2189.
13. U. DOLEGA, *Z. Naturf.* **18a** (1963) 653.
13. P. CHERIN, E. L. LIND and E. A. DAVIS, *J. Electrochem. Soc. Solid State Sci.* **117** (1970) 233.
14. B. D. CULLITY, "Elements of X-Ray Diffraction" 2nd ed. (Addison Wesley, London, 1978).
15. D. W. NILES and F. S. HASSON, *Progress in Photovoltaic* **1** (1993) 132.
16. A. MANY, Y. GOLDSTEIN and N. B. CROVER, "Semiconductor Surfaces" (North Holland, Amsterdam, 1965) p. 307.
17. L. L. KAZMERISKI, W. B. BERRY and C. W. ALLEN, *J. Appl. Phys.* **43** (1972) 3515.
18. R. L. PETRITZ, *Phys. Rev.* **104** (1956) 1508.
19. J. W. ORTON, B. J. GOLDSMITH, J. A. CAPMAN and M. J. POWELL, *ibid.* **53** (1982) 1602.
20. R. K. AHERNKIEL, D. H. LEVI, S. JOHNSTON, W. SONG, D. MAO and A. FISHER, in Proc. 26th IEEE Photovoltaic Conf. 535 (1997).
21. J. TANG, L. FENG, D. MAO, W. SONG, Y. ZHU and J. U. TREFNY, *Mater. Res. Soc. Symp. Proc.* **426** (1996) 227.
22. L. F. ALEN and H. B. RICHARD, "Fundamental of Solar Cells" (Academic Press, 1983).

Received 16 October 2002
and accepted 14 May 2003